Experiments relating to the flow induced by a vibrating quartz tuning fork and similar structures in a classical fluid

D. Schmoranzer,[1] M. Král'ová,[2] V. Pilcová,[1] W. F. Vinen,[3] and L. Skrbek[1]
[1]*Faculty of Mathematics and Physics, Charles University, Ke Karlovu 3, 121 16 Prague, Czech Republic*
[2]*Institute of Physics ASCR, v.v.i., Na Slovance 2, 182 21 Prague, Czech Republic*
[3]*School of Physics and Astronomy, University of Birmingham, Birmingham B15 2TT, United Kingdom*
(Received 12 March 2010; published 28 June 2010)

We report on an experimental study of the behavior of a number of commercially available quartz tuning forks oscillating in a classical cryogenic fluid, in the form of either liquid helium I or gaseous helium, extending our previous studies [M. Blazkova *et al.* Phys. Rev. E **75**, 025302 (2007)]. Measurements of the damping of the oscillations allowed us to deduce the drag on the prong of a fork, as a function of the velocity with which the prong moves, for various sizes of fork and various oscillation frequencies. Transitions to turbulent flow have been identified, and the dependence of the critical velocity, expressed as a dimensionless critical Keulegan-Carpenter number, on the dimensionless Stokes number has been established. These measurements have not allowed us to visualize the flow, so we have carried out visualization experiments with oscillating rods in water, the rod dimensions, and the frequencies of oscillation, being chosen so that the relevant dimensionless parameters are similar to those for the prongs of the forks. Some information about the nature of the instability that leads to turbulence has been obtained in this way, and the results for the critical Keulegan-Carpenter number for the rods in water have been compared with values for the tuning forks in a cryogenic fluid.

DOI: 10.1103/PhysRevE.81.066316 PACS number(s): 47.27.Cn, 47.80.−v, 67.25.B−, 85.50.−n

I. INTRODUCTION

During the past few years a number of papers have reported applications of vibrating piezoelectric quartz tuning forks in the study of cryogenic fluids [1–7]. Such forks are available commercially at little cost since they are made in large numbers as frequency standards for watches. The usual frequency is $2^{15}=32\,768$ Hz, although forks with other frequencies are also available. The forks are normally supplied in cylindrical vacuum-tight metal cans, but removal of this can allows the fork to interact with a surrounding fluid. The piezoelectric properties of the quartz allow both controlled application of a periodic driving force and the measurement of the corresponding response, by purely electrical means. Vibration of a fork at low velocities induces laminar flow in the surrounding fluid, and this allows the fork to be used to monitor the state of the fluid, such as its temperature or pressure, a feature that is particularly valuable in cryogenic applications [2,4]. At higher velocities vibration of the fork can induce turbulent flow, and studies have been reported of the way in which the drag on the prongs of the fork varies with velocity in the transition to fully turbulent flow [3,4,6,7]. This transition has been studied in both gaseous and liquid helium, and in the latter case studies have included both the normal and the superfluid phases. In the case of the superfluid phase we are dealing with quantum turbulence, and the studies have contributed to our understanding of the way in which such turbulence can be generated by a vibrating structure.

Laminar flow induced by vibration of a fork at low velocities seems to be well understood in terms of well-established theory [2,8]. The frequency with which the forks vibrate is such that in either gaseous or liquid helium the viscous penetration depth is small compared with the dimensions of a prong, and there is potential flow outside this penetration depth. The amplitude of the oscillations in drag force, F, per unit length of prong is then related to the velocity amplitude of oscillation, U, through a relation of the form

$$F = \alpha S \rho (\omega \nu)^{1/2} U, \tag{1}$$

where S is the surface area of a prong per unit length; ρ and ν are, respectively, the density and kinematic viscosity of the fluid; ω is the angular frequency of oscillation; and α is a numerical factor, of order unity, which depends on the shape of a prong. The drag force can also be expressed in terms of a drag coefficient C_D,

$$C_D = 2\alpha \frac{S}{A} (\omega \nu)^{1/2} \frac{1}{U}, \tag{2}$$

where A is the projected area of unit length of a prong on a plane normal to its motion and C_D is defined by the equation

$$F = \tfrac{1}{2} \rho A C_D U^2. \tag{3}$$

This paper is concerned with the behavior of a tuning fork in a classical fluid when the velocity is increased through the transition to turbulence. As we shall see, this behavior is interesting in itself, but it is interesting also in connection with the generation of quantum turbulence. A question that arises in the study of quantum turbulence is the extent to which quantum turbulence can mimic classical turbulence. This question has arisen repeatedly in the study of the generation of quantum turbulence by various forms of oscillating structure [9], and it has arisen most recently, and perhaps most vividly, in recent experimental studies of the generation of quantum turbulence by an oscillating tuning fork [6,7]. The pursuit of this question has been hampered, as we shall

see, by the fact that very little seems to be known about the generation of turbulence by a tuning fork, or by similar structures, in a classical fluid.

If we ignore the fact that a tuning fork has two prongs, and that the velocity with which a prong moves varies along its length, we see that the oscillation of such a fork in a fluid must be closely related to the transverse oscillation of a bar of rectangular cross section. Many experimental and theoretical studies have been published relating to the transverse oscillation of a rod of circular cross section in a fluid (for example, [10–15]), with the experiments having included both measurements of the drag coefficient through the transition to turbulence and visual observations of the flow at different stages in this transition. However, to our knowledge no corresponding studies have been made for a bar of rectangular cross section. This paper, which is an extension of our previous studies [3], is a contribution to the filling of this gap in our knowledge. Our measurements include studies of the drag-force–velocity relationship for a range of tuning forks in helium, supplementing the results presented in [3], together with visual observations of the flow induced in water by transverse oscillations of a rectangular bar, for which the dimensionless parameters are chosen to match those relevant to the tuning forks. Our results suggest that there may be significant differences between the behaviors of a rod of circular cross section and that of our rectangular bars, although we cannot be sure of the reason and further experiments are clearly required.

In presenting our experimental results we shall use the dimensionless parameters that are commonly used in the classical literature. The drag will be described by the dimensionless drag coefficient, defined by Eq. (3). At a finite frequency this drag coefficient must be a function of two independent dimensionless parameters, which we take to be the Keulegan-Carpenter number, defined by the equation

$$K_C = \frac{2\pi a}{d}, \tag{4}$$

and the Stokes number, defined by the equation

$$\beta = \frac{\omega d^2}{2\pi\nu}, \tag{5}$$

where a is the amplitude of oscillation of the structure and d is a characteristic dimension. In terms of these dimensionless parameters Eq. (2) becomes

$$C_D = (8\pi)^{1/2}\alpha\frac{S}{A}\beta^{-1/2}K_C^{-1}. \tag{6}$$

At velocities exceeding those at which there is laminar flow the form of Eq. (6) becomes generally more complicated, although it is often the case that in the limit of very large K_C the drag coefficient tends to a constant value of order unity, which we denote by Γ.

II. EXPERIMENTAL RESULTS: DRAG ON THE VIBRATING TUNING FORKS

Details of the quartz forks that we have studied are summarized in Table I, with the dimensions being defined in Fig. 1. The surfaces of the forks are rough on a scale of a few microns, as shown in Fig. 1. The way in which our experimental results have been obtained was described in earlier papers.

TABLE I. Description of quartz forks.

Fork	Frequency (kHz)	L (mm)	T (mm)	W (mm)	D (mm)
A1	32	3.71	0.42	0.35	0.21
B1	32	3.65	0.68	0.46	0.18
C3	32	2.51	0.25	0.10	0.13
U1	4	19.70	2.20	0.80	
U2	8	9.50	0.45	0.90	0.50
L2	32	2.17	0.21	0.10	0.12
L1	32	2.17	0.21	0.10	0.12
K1	32	3.9	0.39	0.28	

A typical plot of observed drag coefficient against Keulegan-Carpenter number, for a fixed value of Stokes number, is shown in Fig. 2. We see that there is a smooth (monotonic) transition between the laminar behavior, described by Eq. (6), and a limiting constant value $C_D=\Gamma$ at high velocity, where the constant Γ is close to unity. We find that this smooth transition can be represented to a good approximation by the equation

$$C_D = (8\pi)^{1/2}\alpha\frac{S}{A}\beta^{-1/2}K_C^{-1} + \Gamma, \tag{7}$$

which describes all solid lines in Fig. 2.

We note that this smooth variation is different from that observed with a circular cylinder, where C_D often varies with K_C in an oscillatory way in the region of the transition to turbulent flow [10]. Furthermore, there is evidence that the limiting value of the drag coefficient for a circular cylinder, although of order unity, does in fact decrease systematically and significantly with increasing β. This suggests that the physical processes occurring in the transition region may be different in character in the two cases, although—as we discuss later—part, at least, of the difference might be due to the fact that the transverse velocity with which a fork vibrates must vary along its length.

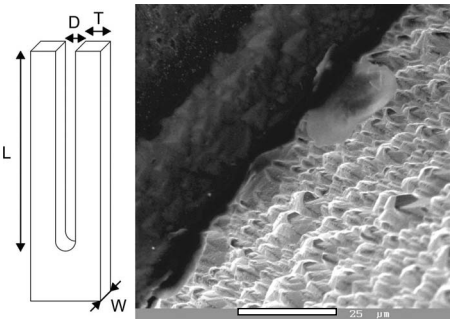

FIG. 1. Schematic sketch of a quartz tuning fork and a micrograph of the surface of tuning fork A1 (the marker is 25 μm long).

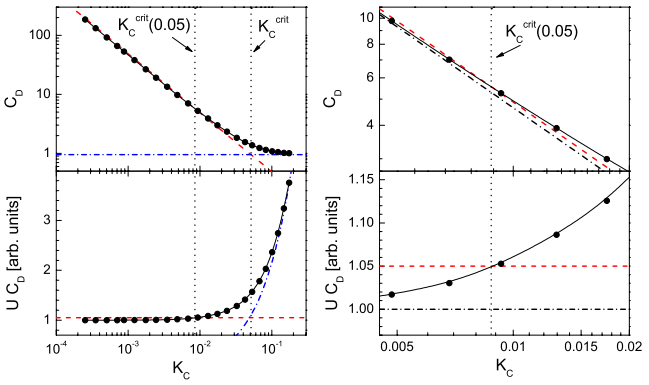

FIG. 2. (Color online) Upper left panel: the observed drag coefficient plotted against Keulegan-Carpenter number for a 32 kHz fork of type B1. Lower left panel: the same drag coefficient multiplied by velocity (normalized to unity)—this quantity indicates a departure from linearity more clearly. The (blue) dashed-dotted line indicates the fully turbulent drag. The right panels show detailed view of the departures from linear regime indicated by the (black) dashed-dotted line. In all panels the 5% departure criterion is marked by the (red) dashed line and the critical Keulegan-Carpenter numbers are marked with vertical black dotted lines.

We shall be interested in defining a critical Keulegan-Carpenter number $K_C^{\rm crit}$ associated with this transition. It is tempting to define this number as that at which the two terms on the right-hand side of Eq. (7) are equal, so that

$$K_C^{(\rm crit)} = (8\pi)^{1/2}\frac{\alpha}{\Gamma}\frac{S}{A}\beta^{-1/2}. \tag{8}$$

We note that this form implies that the corresponding critical velocity scales as $(\omega\nu)^{1/2}$ for a given oscillating structure, a form of scaling that was noted in Ref. [3]. However, this scaling is an automatic consequence of the limiting forms of C_D in the laminar and fully turbulent regimes; it has no special physical significance in the sense that the critical velocity does not correspond to any special change in the character of the flow [6]. Of more significance is the value of K_C at which the first instability appears in the laminar flow. Unfortunately, since the observed variation of C_D is quite smooth, it is not possible to identify this critical condition. The best we can achieve is to identify the value of K_C, $K_C^{\rm crit}(x)$, at which C_D differs from its laminar value by an arbitrary factor $(1+x)$, where $x \ll 1$.

In Figs. 3 and 4 we show plots of the observed values of $K_C^{\rm crit}$ and $K_C^{\rm crit}(0.05)$ against Stokes number. We see from Fig. 3 that $K_C^{\rm crit}$ varies with Stokes number as $\beta^{-1/2}$, in accord with Eq. (8). We see from Fig. 4 that $K_C^{\rm crit}(0.05)$ also varies with Stokes number as $\beta^{-1/2}$, within the (considerable) experimental error. This strongly suggests (but perhaps does not yet conclusively prove) that the critical Keulegan-Carpenter number at which the laminar flow first becomes unstable also varies with Stokes number as $\beta^{-1/2}$. In this respect an oscillating fork seems to behave differently from an oscillating rod of circular cross section, for which the critical Keulegan-Carpenter number at the first onset of instability (the Honji instability [12], discussed below) varies less rapidly with

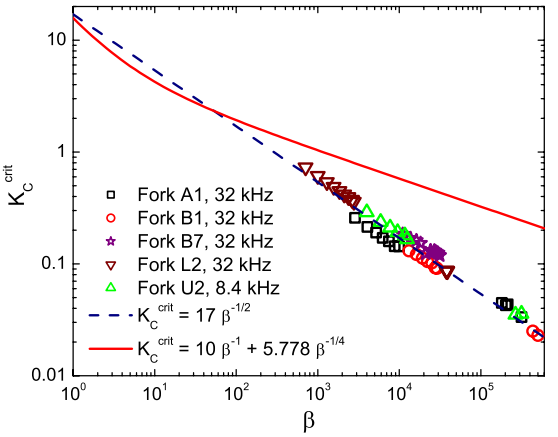

FIG. 3. (Color online) The critical Keulegan-Carpenter number $K_C^{\rm crit}$ plotted against Stokes number β for different forks as indicated, vibrating in normal liquid ^{4}He and in cold pressurized helium gas at liquid-nitrogen temperature. The solid (red) line represents the expected instability for circular cylinders and the (blue) dashed line represents the observed square-root behavior as indicated.

Stokes number (as $\beta^{-1/4}$ for large β [10]). This less rapid variation with β may be related to the fact, noted above, that the value of Γ seems to decrease systematically with increasing β.

III. VISUALIZATION

These experimental results leave unanswered a number of important questions. To what extent is the behavior of a fork influenced by the sharp corners on the prongs and by roughness of the surface of a prong? To what extent is it influenced by the close proximity of two prongs and the nonuniform transverse velocity of a prong? And what is the nature of the first instability as the Keulegan-Carpenter number is increased?

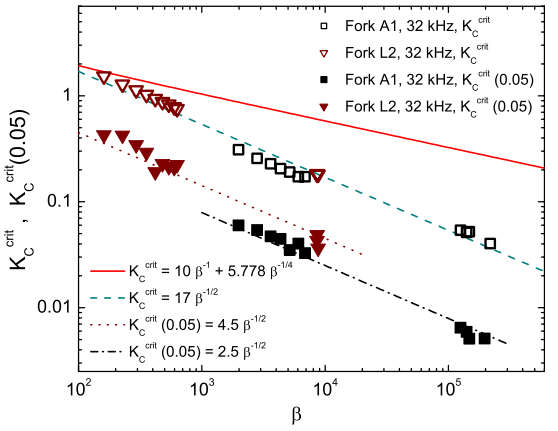

FIG. 4. (Color online) The critical Keulegan-Carpenter numbers, $K_C^{\rm crit}$ and $K_C^{\rm crit}(0.05)$, plotted against Stokes number for different forks as indicated, vibrating in normal liquid ^{4}He and in cold pressurized helium gas at liquid-nitrogen temperature. The (red) solid line represents the expected instability for circular cylinders; the other lines are the individual observed square-root dependences.

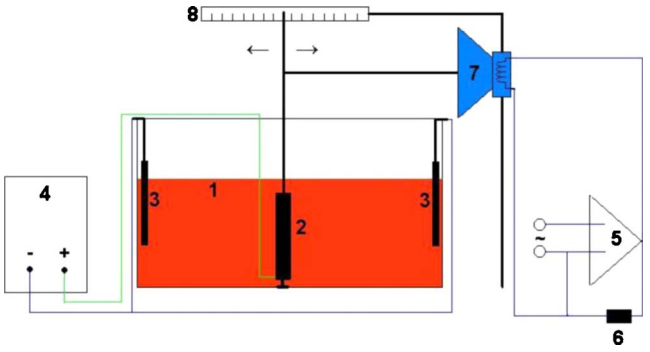

FIG. 5. (Color online) Schematic diagram of the apparatus used to visualize the flow produced by an oscillating bar in water. For a detailed description, see the text.

It is difficult to answer these questions with the forks themselves. They cannot easily be modified to answer the first two questions. Establishing experimentally the nature of the first instability requires a visualization of the flow, for which the required technique does not exist for such a small structure immersed in a cryogenic fluid. We have therefore started to investigate the behavior of large metal rods of rectangular cross sections oscillating in water, aiming by suitable scaling at ranges of values of K_C and β similar to those relevant to the forks. Ideally, we should have measured the drag coefficients for such systems, but as yet we do not have the equipment necessary for such measurements. But we have attempted to visualize the flow, using both the Baker solution technique [16] and a Kalliroscope solution [17].

A. Experimental technique

The apparatus based on the Baker *p*H technique is shown schematically in Fig. 5. Approximately 25 l of Baker solution composed of water, small concentrations of NaOH and HCl, and thymol blue *p*H indicator (labeled 1) were contained in a tank of dimensions $20\times30\times25$ cm^3. The oscillating rod (2) was pivoted at the base of the tank with a spherical knob fitting into a Teflon holder. Oscillation of the rod about the pivot in a vertical plane was driven via two thin rods by a large bass loudspeaker (7), driven by the oscillator (5), over a range of frequencies from 1 to 12 Hz. The loudspeaker was used in its linear mode, so that the amplitude of oscillation was proportional to the applied ac signal. In the experiment, the oscillating rod could move along its sides only and was pivoted at its lower end in order for its motion to be similar to that of a prong of a tuning fork. The surface of the rod was biased by a dc voltage of 10–15 V relative to the brass electrodes (3), in accordance with the recipe given in Ref. [16]. When the dc bias voltage is applied, an electrochemical reaction starts on the surface of the rod, affecting the concentrations of the dissociated ions locally thus increasing the local *p*H, and forcing the *p*H indicator in the vicinity of the rod to change its color from orange-red to dark blue. This "ink" then freely drifts in the liquid, marking its flow pattern accurately at low velocities up to about 5 cm/s. The same tank, without the electrodes, was used for experiments with the Kalliroscope solution, which outlines the flow pattern via small reflective platelets contained in it. Calibration of the displacement and velocity of the rod was carried out with a video camera that recorded the position of the top of the system of thin rods as a function of time relative to the scale (8).

B. Existing observations

Before we present our own observations of the flow of water round our oscillating rods, we shall describe existing observations of flow round an oscillating rod of circular cross section [10,12], together with one previous unpublished observation of the flow round an oscillating rod of square cross section [18]. Comparison between the different observations will prove instructive.

An important and detailed study of the flow of water round a rod of circular cross section oscillating in a direction at right angles to its length was reported by Honji [12]. Similar observations, together with corresponding measurements of the drag coefficient versus Keulegan-Carpenter number, were reported by Sarpkaya [10]. The observed flows can be summarized in a slightly oversimplified way as follows. At a small velocity (or K_C), within the laminar regime, oscillation leads to not only an oscillating boundary layer, but also to a steady streaming flow [19,20]. The streaming flow is two dimensional in the sense that the streaming velocity points in a direction normal to the length of the rod. It arises from a nonlinear effect when flow in the oscillating boundary layer varies with position in the direction in which the flow takes place; for the case of an incompressible fluid the equation of continuity demands that there must then be some flow normal to the plane of oscillation. The relevant theory was given by Schlichting and was discussed by Batchelor [21]. At a higher Keulegan-Carpenter number the flow starts to exhibit a three-dimensional structure involving mushroom-shaped vortices moving away from the surface (see, for example, Ref. [12], Fig. 10). It is now accepted that this flow arises from an instability of the flow in the boundary layer when the rigid boundary has convex curvature, with the instability leading to the generation of Taylor-Görtler vortices [15]. As long as these vortices remain in the thin boundary layer they are hard to see, but the steady streaming flow causes them to be swept away from the cylinder, so that they appear very clearly in the form of the mushroom-shaped vortices to which we have referred. Theory [15] leads to the prediction that the critical Keulegan-Carpenter number at which the Taylor-Görtler vortices are formed (the initial instability) is given in the limit of large β by

$$K_C^{(\mathrm{crit})} = 5.778\beta^{-1/4}. \tag{9}$$

This dependence on β, to which we have already referred, has been verified experimentally [10].

The only study of flow induced by the transverse oscillation of a rod of rectangular cross section of which we are aware has been carried out by Hershberger and Donnelly [18]. They used Kalliroscope to visualize the flow, and their bar oscillated with a velocity amplitude that was uniform along its length. They did not report any observation of steady streaming at low velocities, but they did observe

FIG. 6. (Color online) A photograph of the (brass or stainless steel) rods of square cross section that we have studied. They have cross sections of 5×5, 3×3, 2×2 (with rounded corners), 2×2, and 1×1 cm^2.

mushroomlike vortices formed along the whole length of the bar at higher velocities, with the vortices being arranged in a regular pattern along the length of the bar. They did not carry out a complete study, and the precise location of the mushroom vortices remains unclear.

C. Present observations

Photographs of the rods that we have studied are shown in Figs. 6–8. The 2×2 cm^2 rod with rounded edges showed no transition within the range of velocities available to us. All the others showed a transition in which vortex motion leaves the surface, as shown in the typical photograph reproduced in Fig. 9. These vortices are not arranged in the regular pattern along the rod as observed by Hershberger and Donnelly, and they first appear at the top of the rod (we neglect structures shed by the upper edge). On increasing the amplitude of oscillation further above the critical value, vortices start appearing further away from the top of the rod. These features are consistent with the fact that the transverse velocities with which our rods move are not uniform along their lengths, but increase from zero at the bottom to a maximum value at the top of each rod. We identify a critical velocity as that velocity at the top of a rod at which the first vortices are observed to be produced 0.5–1 cm below the upper edge. The corresponding critical Keulegan-Carpenter numbers are plotted against the Stokes number in Fig. 10.

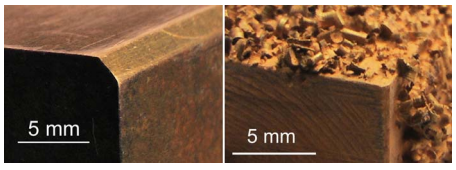

FIG. 7. (Color online) Left: the detail of the trimmed edge (after the second trimming) of the 3×3 cm^2 brass rod. Right: the detail of the roughened gold-plated surface of the 2×2 cm^2 brass rod.

FIG. 8. (Color online) A photograph of two brass cylinders of square cross section 2×2 cm^2. The surface of the lower one was roughened by soldering small brass shavings to it; this surface was then electrochemically cleaned and gold plated.

We see from Fig. 10 that most of the data are consistent with a critical Keulegan-Carpenter number K_C^{crit} that is proportional $\beta^{-1/2}$, as was the case with the tuning forks. The

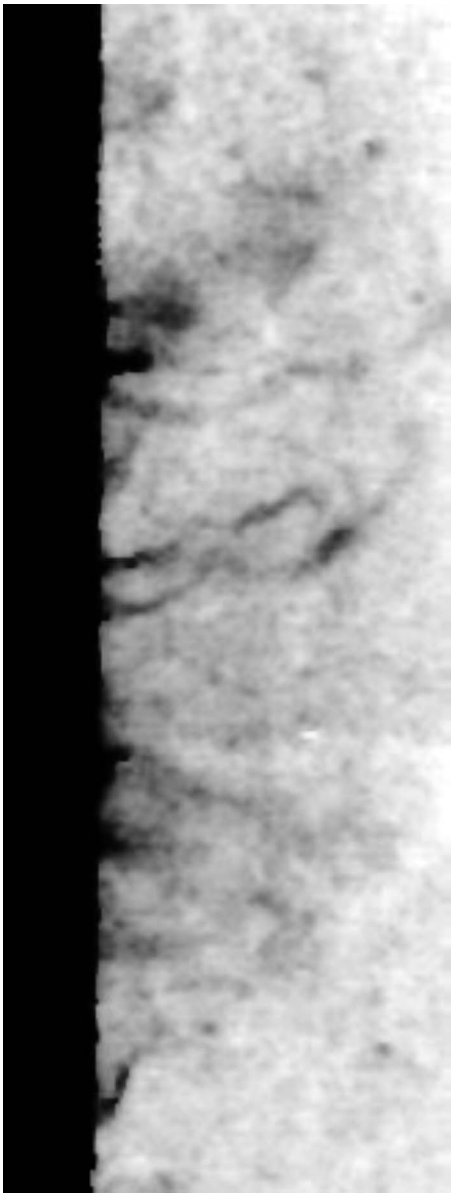

FIG. 9. A photograph showing a typical pattern of vortices produced by an oscillating rod of cross section 3×3 cm^2 at a velocity amplitude well above the transition.

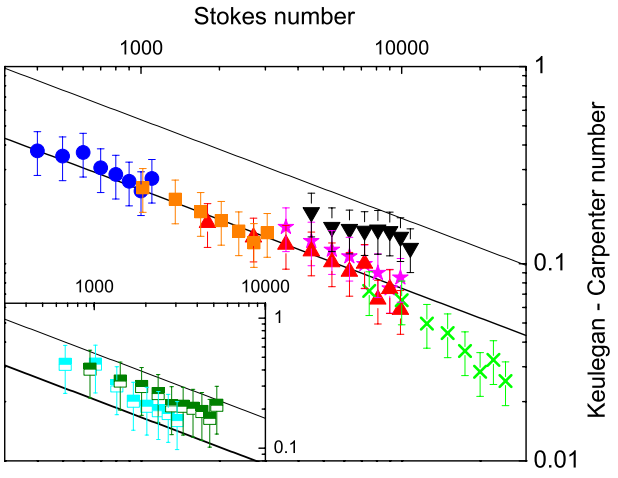

FIG. 10. (Color online) The critical Keulegan-Carpenter number plotted against Stokes number for various rods of square cross section oscillating in water. All the data were obtained by visualization, and relate to the first appearance of vortices being shed by the rod about 0.5 cm below the upper edge. The data in the main graph were obtained with the Baker *p*H technique; those in the inset were obtained by the Kalliroscope technique. In the main graph, filled (blue) circles, filled (orange) squares, filled (red) triangles, and (green) crosses represent the data observed with rods of 1×1, 2×2, 3×3, and 5×5 cm^2 square cross sections, respectively; (magenta) stars and (black) triangles show how the critical Keulegan-Carpenter number changes when the sharp edges of the 3×3 cm^2 rod are trimmed successively. The inset shows the critical Keulegan-Carpenter number for the 2×2 cm^2 rod, obtained with the Kalliroscope technique before [upper (dark green) symbols] and after [lower (cyan) symbols] roughening of the surface. The dotted straight line corresponds to $K_C^{\rm crit}=17\beta^{-1/2}$ (c.f. Fig. 3) and the solid line is $K_C^{\rm crit}=7.5\beta^{-1/2}$.

only exception is the rod with cross section 5×5 cm^2, the anomalous behavior of which may be associated with the fact that its length is not sufficiently large compared with its width to ensure that end effects are not important. We note that the absolute values of $K_C^{\rm crit}$ for our rods, for a given value of β, are closely similar to those of $K_C^{\rm crit}(0.05)$ for the tuning forks, suggesting that our "5% criterion" in the latter case does indeed indicate reasonably accurately the first instability, as observed with the bars in water.

To check the influence of sharpness of the edges on $K_C^{\rm crit}$ experimentally, we have successively trimmed the edges of the 3×3 cm^2 rod. This trimming has been done very accurately using a milling cutter (see Fig. 7), so that the size of the trim was 1 and 2 mm, respectively, after the first and the second trimming. The fact that $K_C^{\rm crit}$ for the rod of cross section 3×3 cm^2 is increased when the sharp corners are trimmed suggests that the onset of the first instability in the laminar flow is associated with these sharp corners. In contrast with a rod of circular cross section, the overall width of the rod may therefore be irrelevant to this instability, and this difference may account for the different dependence of $K_C^{\rm crit}$ on β in the two cases; instead of the overall width, what may be important is either the radius of curvature at the sharp edge or the radius of curvature of the outer surface of the viscous penetration depth, whichever is the larger. The fact that roughening the surface of the rod of cross section 2×2 cm^2 has such a small effect is surprising, in view of the fact that the scale of the roughness is larger than the viscous penetration depth. It does, however, suggest that surface roughness may not be an important factor in the behavior of the tuning forks. Our experiments do not tell us whether the proximity of the two prongs of a tuning fork is important.

IV. CONCLUSIONS

Commercially available quartz tuning forks are being used increasingly in various applications at cryogenic temperatures. We have measured the damping of the oscillations of a range of such forks in classical cryogenic fluids (helium I and helium vapor), and we have observed the transition from laminar to turbulent flow. The critical Keulegan-Carpenter number $K_C^{\rm crit}$ corresponding to the initial departure from laminar behavior, and so to the initial instability of laminar flow, is found probably to be proportional to $\beta^{-1/2}$, where β is the Stokes number. In order to throw more light on the behavior of these forks, we have carried out experiments on rods of square cross section (to mimic a prong of a fork) oscillating in water, with the dimensions and frequency of oscillation being chosen to correspond to values of the relevant dimensionless parameters that are close to those for the forks. Visualization of the flow of the water suggests that, as is known to be the case with rods of circular cross section, the transition to turbulence involves an initial instability within the viscous penetration depth, with the resulting vortex motion being dragged away from the surface by the steady streaming that is known to be associated with oscillatory motion of a curved structure in a classical fluid. Values of $K_C^{\rm crit}$ obtained from the visual observations display the same dependence on β as was observed with the tuning forks. When the sharp corners of a rod were trimmed the value of $K_C^{\rm crit}$ was found to increase significantly. This suggests that the initial instability is associated with the small radius of curvature at these corners. The dependence of $K_C^{\rm crit}$ on β that we observe ($\beta^{-1/2}$) is different from that reported for rods of circular cross section ($\beta^{-1/4}$ at high velocities). We suggest that this difference arises because the relevant radius of curvature is the overall radius in the case of a rod of circular cross section, while it is the radius of curvature associated with the corners of a rod of square cross section, with this latter radius being the actual radius or the radius of curvature of the outer part of the viscous penetration depth, whichever is the larger. In the case of a rod of circular cross section the drag coefficient tends to oscillate in value with increasing β, in the neighborhood of the transition, while the drag coefficient that we observe with our forks varies smoothly. While this difference may reflect a different type of flow, it may also be associated, at least in part, with the fact that the velocity with which a prong of one of our forks moves varies along its length. Roughening the surface of one of our rods was observed, surprisingly, to have little effect on the value of $K_C^{\rm crit}$.

ACKNOWLEDGMENTS

We are grateful to O. Kolosov and B. Studer for providing some of quartz tuning forks used in this work, to R. Hershberger and R. J. Donnelly for showing us the results of their research prior to publishing, and to L. Doležal for skillful manufacturing of the visualization equipment. This research was supported by research plans MS 0021620834 and by GAČR Contract No. 202/08/0276.

[1] D. O. Clubb, O. V. L. Buu, R. M. Bowley, R. Nyman, and J. R. Owers-Bradley, J. Low Temp. Phys. **136**, 1 (2004).
[2] R. Blaauwgeers *et al.*, J. Low Temp. Phys. **146**, 537 (2007).
[3] M. Blažková, D. Schmoranzer, and L. Skrbek, Phys. Rev. E **75**, 025302 (2007).
[4] M. Blažková *et al.*, J. Low Temp. Phys. **148**, 305 (2007); **150**, 525 (2008).
[5] E. M. Pentti, J. T. Tuoriniemi, A. J. Salmela, and A. P. Sebedash, J. Low Temp. Phys. **150**, 555 (2008).
[6] M. Blažková, D. Schmoranzer, L. Skrbek, and W. F. Vinen, Phys. Rev. B **79**, 054522 (2009).
[7] D. I. Bradley *et al.*, J. Low Temp. Phys. **157**, 476 (2009).
[8] L. D. Landau and E. M. Lifshitz, *Fluid Mechanics*, 2nd ed. (Butterworth-Heinemann, Oxford, 1987).
[9] L. Skrbek and W. F. Vinen, in *Progress in Low Temperature Physics*, edited by M. Tsubota and W. P. Halperin (Elsevier, New York, 2009), Vol. XVI, Chap. 4.
[10] T. Sarpkaya, J. Fluid Mech. **165**, 61 (1986).
[11] M. Tatsuno and P. W. Bearman, J. Fluid Mech. **211**, 157 (1990).
[12] H. Honji, J. Fluid Mech. **107**, 509 (1981).
[13] C. H. K. Williamson, J. Fluid Mech. **155**, 141 (1985).
[14] E. D. Obasaju, P. W. Bearman, and J. M. R. Graham, J. Fluid Mech. **196**, 467 (1988).
[15] P. Hall, J. Fluid Mech. **146**, 347 (1984).
[16] D. J. Baker, J. Fluid Mech. **26**, 573 (1966).
[17] www.Kalliroscope.com/juices/rheoscopic_fluids.htm
[18] R. Hershberger and R. J. Donnelly (private communication).
[19] H. Schlichting, Phys. Z. **33**, 327 (1932).
[20] H. Schlichting and K. Gersten, *Boundary-Layer Theory* (Springer, New York, 1996).
[21] G. K. Batchelor, *An Introduction to Fluid Dynamics* (Cambridge University Press, Cambridge, England, 1967).